

Wave and Wind Induced Responses of the Semisubmersible Wind Energy and Flap-type Wave Energy Converter Based on Experiments

Constantine Michailides, Zhen Gao and Torgeir Moan
Department of Marine Technology, Norwegian University of Science and Technology (NTNU)
Trondheim, Norway

ABSTRACT

This paper deals with a study of wave and wind induced responses of the combined energy concept SFC in operational and survival conditions based on experimental data. The measured responses that are studied include motions of the semisubmersible, rotation of the flap-type WECs, tension of mooring lines, internal loads of the arms of the WECs, bending moment at the base of the wind turbine tower and produced power by WECs. The effect of both the change of the mean heeling angle of the SFC and the aerodynamic damping are studied. The effect of the wind loading in structural responses of different parts of WECs of SFC considering a constant and uniform wind field is small.

KEY WORDS: Semisubmersible wind energy and Flap-type wave energy Converter, Floating offshore wind turbines, Wave energy converters, Offshore combined energy concepts, Physical model testing.

INTRODUCTION

The technology in offshore renewable energy sector which can be considered mature enough is the Offshore Wind Turbines (OWTs) technology. The Levelised Cost Of Energy (LCOE) of OWTs in 2013 is in the range of 130-330 USD/MWh (World Energy Council, 2013). The cost of OWTs is the main handicap for their further utilization. In order to reduce the cost of generated power, the development of large wind turbines with high rated power in deep seas is considered as an efficient potential direction. For deep seas the use of Floating type OWTs (FOWTs) is considered as the most cost-efficient solution. Different floating support platform configurations are possible for use with FOWTs (Jonkman and Matha, 2011). A major type of support configuration is the semisubmersible platform consisting of three columns that are connected with the use of braces (Roddi et al., 2010). Alternatively, the columns of the semisubmersible platform can be connected by pontoons with large dimensions without braces (Olav Olsen, 2015; Karimirad and Michailides, 2015). Three column braceless semisubmersibles have been deployed in the past in the offshore oil industry; results based on physical model test and full-scale tests accounting for free-surface and water depth effects are comprehensively examined by Chung (1976) and Chung (1994).

Ocean waves are an extremely abundant and promising resource of alternative and clean energy. Many different types of Wave Energy Converters (WECs) have been proposed. The first patent of a WEC has been registered in 1799 in France by a father and a son named

Girard (Michailides, 2015). Unfortunately the technology of WECs cannot be considered mature yet for large-scale commercial deployment. The LCOE of WECs in 2013 is in the range of 280-1000 USD/MWh (World Energy Council, 2013). WECs can be deployed in multi-purpose floating structures (Michailides and Angelides, 2015).

It might be beneficial to combine offshore renewable energy systems of different technology into one floating platform. Possible advantages as a result of the use of offshore combined concepts are: (a) increase of the energy production per unit area of space, (b) decrease of the cost per MWh production of energy of a pure OWT or a pure WEC, (c) decrease of the cost related with the required electric grid infrastructure and (d) decrease of the cost related with operation (e.g. installation) and maintenance (e.g. inspection). Recently, EU research projects have been introduced to accelerate the development of offshore combined energy systems.

In the EU project MARINA Platform (2015) three combined concepts have been selected and studied both numerically and experimentally. These three combined concepts are the Semisubmersible wind energy and Flap-type wave energy Converter (SFC) (Michailides et al., 2014), the Spar Torus Combination (STC) (Muliawan et al., 2013) and an array of oscillating water columns in a V-shaped concrete large floating platform and one wind turbine combination (O'Sullivan and Murphy, 2013). The combined concept SFC consists of a braceless semisubmersible floating platform, a 5 MW wind turbine, three rotating flap-type WECs and three catenary mooring lines (Fig. 1).

As far as physical model testing of OWTs is concerned, there are different techniques for the physical modeling of the rotor, tower and thrust force. One important uncertainty related to interpretation of the test results is the scaling effect (e.g. Müller et al., 2014). The rotor of the wind turbine can be simplified as a disk providing a drag force (Roddi et al., 2010) or as a controlled fan providing an active force

type WECs (Table 1). Each WEC consists of one fully submerged flap with elliptical shape, two cylindrical shaped arms and one rotating shaft (axis of rotation). The flap has been built by synthetic foam, while the arms and the shaft by titanium. The upper point of the flap in its mean position is 2 m and 3.25 m below the Mean Water Level (MWL) for the functionality and survivability model, respectively. The lower point of the flap is 15 m above the pontoon of the platform for both models. Each arm is rigidly connected with the flap at the higher end. At the lower end the arm is rigidly connected with a shaft that is founded to the pontoon of the platform in two low friction bearings. Additionally, the shaft through a third low bearing is inserted into the adjacent side column of the platform and is connected with a PTO

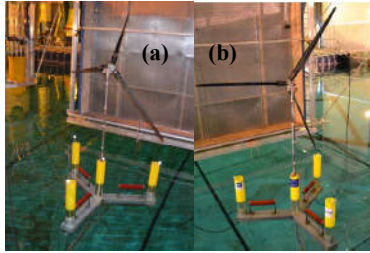


Figure 3. Survivability (Fig. 3a) and functionality (Fig. 3b) physical models of SFC

configuration, which is used to physically model the linear PTO of the WEC (only for the functionality model). The PTO configuration consists of a lower and an upper pulley, a timing belt, two tensioners and a linear mechanical rotary damper. The damping coefficient of the mechanical rotary damper, C_{PTO} , is manually adjusted prior to the tests. The instantaneous produced power of each WEC is:

$$P(t) = C_{PTO} \dot{\theta}(t)^2 \quad (\text{Eq. 1})$$

where $\dot{\theta}(t)$ is the velocity of the rotation of the shaft. It is noted that the tests are performed for representative operational and survival conditions; the experimental investigation of the fatigue life of the WECs is out of the scopes of this work based on an experimental study.

Table 1. Scaling factors for different variables

Variables	Scale factor	
	λ	
Linear dimensions (length, height, width, wave height etc)	λ	50
Mass, Force	λ^3	125,000
Time, Velocity	$\lambda^{0.5}$	7.07
Moment	λ^4	6,250,000
Produced power by WECs	$\lambda^{3.5}$	883,883.5

As far as the modelling of the wind turbine, a redesigned small-scale rotor has been used as compared to the NREL 5 MW reference wind turbine (Jonkman et al. 2009). Since the same Reynolds number cannot be achieved in the physical model, the blades of the wind turbine are redesigned in order to produce the correct thrust force relative to Froude laws of similitude. In Table 2 structural properties of different parts of the wind turbine that are used for the survivability and functionality tests of SFC are tabulated. It should be noted that in Table 2 the value of the tower bending mode frequency is obtained from the appropriate hammer tests of the complete structure in the basin. As far as the tower of the wind turbine (the properties of the tower does not match with the NREL 5MW reference wind turbine), initially a study was performed in order to select the properties of the tower. The parameters constraining the selection of the properties of the tower are: (a) the first bending frequency of the tower has to be kept in the 'soft-stiff range' between 1P and 3P and if possible more

close to the 3P value, (b) the total tower mass has to be close to 226,250 kg in order the total mass of the redesigned wind turbine to be equal with the total mass of the reference wind turbine and (c) the external radius of the tower should be as small as possible. Details with regard to the design of the wind turbine exist in Courbois (2013).

In Fig. 4 main dimensions of different parts of the survivability model of SFC are depicted in full scale. In Table 3 the properties of the main components of the SFC are in full scale values. In Fig. 5 different parts and sensors of the physical model of SFC are depicted. The sampling rate of all the sensors is equal to 120 Hz.

As far as the mooring lines, three catenary mooring lines made by inox chain are used with weight in air per unit length equal to 152.5 kg/m. The horizontal stiffness of each mooring line is 563 N/m, while the vertical stiffness is 167 N/m. The pretension of the mooring lines at the fairlead is equal to 1,779 kN. The diameter of the chain that was used during the experiments is 0.1 m. The radius of the circle that the anchors of the mooring lines are form is 855 m.

Based on decay tests the natural periods of surge, heave and pitch motion of the semisubmersible platform and rotation of WEC2 of the survivability model, $T_{exp,surv}$, and of the functionality model, $T_{exp,fun}$, are tabulated in Table 4.

Table 2. Structural properties of different parts of wind turbine

Variables	SFC
Blade length [m]	61.15
Blade mass [kg]	16,875
Blade flapwise flexible mode [Hz]	1.032
Nacelle mass [kg]	243,750
Shaft tilt [°]	5
Hub mass [kg]	79,375
Vertical distance of hub to the MWL [m]	90
Horizontal distance of hub to the tower [m]	4.98
Tower mass [kg]	226,250

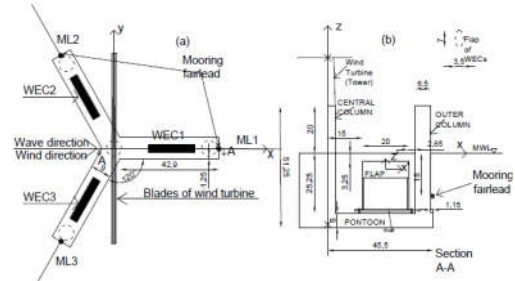


Figure 4. Plan view (Fig. 4a) and side view (Fig. 4b) of SFC

Table 3. Structural properties of main components of functionality model of SFC

Variables	SFC
COG of the whole SFC (x,y,z) [m]	(0,0,-18.35)
I_{xx} (kg*m ²) of the platform	11,445,542,000
I_{yy} (kg*m ²) of the platform	11,445,542,000
I_{zz} (kg*m ²) of the platform	9,772,627,000
Mass of each flap [kg]	100,000
Displacement of each flap [kg]	395,000
WEC $I_{x'x'}$ local coordinate system (kg*m ²)	656,250
WEC $I_{y'y'}$ (kg*m ²)	4,496,875
WEC $I_{z'z'}$ (kg*m ²)	4,168,750

COMPARISONS OBTAINED WITH THE SFC SURVIVABILITY MODEL

Table 4. Natural periods of surge, heave, pitch and rotation of WEC2

Degree of freedom	$T_{exp,surv}$ (sec)	$T_{exp,fin}$ (sec)
Surge	114.76	113.066
Heave	26.445	26.233
Pitch	34.789	34.548
Rotation of WEC2	14.778	14.483

The environmental conditions that comparisons of the wave-induced responses with wave-wind-induced responses of the survivability model of SFC are performed are presented in Table 5; the conditions correspond to irregular waves without or with wind loading. For the survivability model regular wave tests have been conducted only for wave with wind loading and are not included in the present paper. EEC1 ~ EEC4 correspond to tests with wave only loading and EEC1W ~ EEC4W correspond to tests with wave and wind loading.

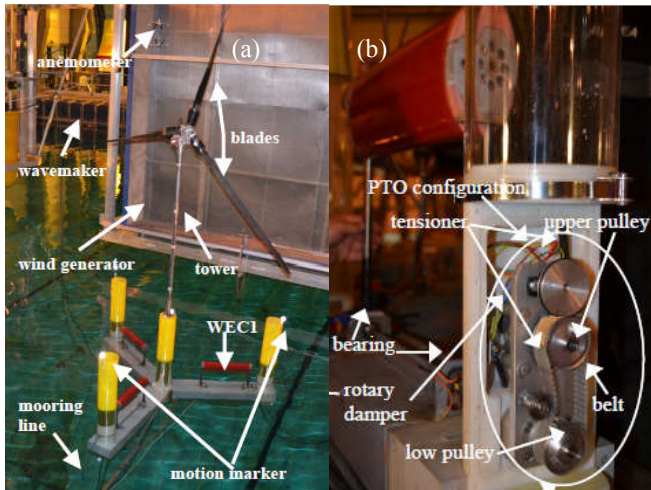


Figure 5. Survivability model of SFC placed into the basin (Fig. 5a) and PTO configuration of functionality model of SFC (Fig. 5b)

The turbulence intensity of the measured wind data is 0.102, 0.108, 0.101 and 0.092 for EEC1W, EEC2W, EEC3W and EEC4W, respectively. A comparison of spectra of wave elevation in WG1 for extreme environmental conditions is plotted in Figure 6. As far as the extreme environmental conditions that are concerned, the sites no. 3 and 14 of the MARINA platform project are selected (Li et al., 2015). Two different conditions (condition with maximum wind speed, U_w , or with maximum significant wave height, H_s) for each site considering the 50 year return value are examined. It should be noted that the mean wind speed here refers to the wind speed at the reference height of 10m above the mean water level and the wind speed at the hub height (90m above the mean water level) is derived based on a power-law wind profile. The duration of the tests is 4,100 sec. The first 495 sec of the tests have been eliminating before the post processing of the measured data.

Table 5. Examined extreme environmental conditions

Extreme conditions/Test case	H_s (m)	T_p (sec)	U_w (m/sec)
EEC1	8.8	14.8	-
EEC2	13.5	15	-
EEC3	11.5	15.7	-
EEC4	15.3	15.5	-
EEC1W	8.8	14.8	27.9
EEC2W	13.5	15	33.3
EEC3W	11.5	15.7	24.3
EEC4W	15.3	15.5	31.4

In Tables 6, 7 and 8 the statistical values of standard deviation, std, maximum, max, and mean values of the experimental data for surge, heave, pitch and rotation of WEC2 for all the examined extreme conditions exist. The statistical values are calculated by the one hour time series of measured data. As far as the std value, the effect of the wind loading is insignificant for the motions of the platform. The wind loading results in a small increase of the standard deviation of the rotation of the WEC2. With regard to the maximum value of the motions, the wind loading results to the increase of the rotation of the WEC2 and to the increase of the surge motion of the platform mainly for EEC2 and EEC4 conditions. As far as the mean value, the effect of the wind loading is obtained mainly for surge and pitch motions of the platform and for EEC2W and EEC4W conditions. The mean of the WEC2 rotation is zero. The largest maximum value that is measured experimentally is 15.095 m for surge motion, 5.53 m for heave motion, 4.911 deg for pitch motion and 24.380 deg for rotation of WEC2 for EEC4W, EEC4, EEC4W and EEC4W conditions, respectively. It must be noted that the mean value of the thrust force (shear load at the top of tower) is equal to 24.19 kN, 34.36 kN, 201.4 kN and 30.56 kN for EEC1W, EEC2W, EEC3W and EEC4W, respectively.

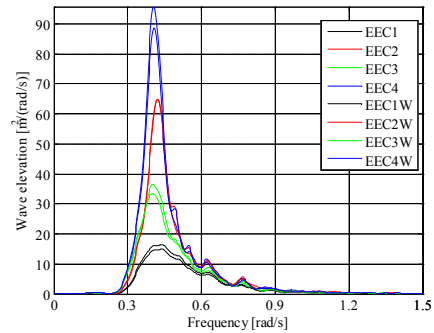


Figure 6. Comparison of spectra of wave elevation in WG1 for extreme environmental conditions

Table 6. Statistical standard deviation value of motions for extreme conditions

Motion	EEC1	EEC1W	EEC2	EEC2W
Surge (m)	1.520	1.525	2.510	2.485
Heave (m)	0.880	0.875	3.480	1.385
Pitch (deg)	0.4861	0.4834	0.7591	0.7122
WEC2 rot. (deg)	5.9793	6.1210	7.0961	7.0903
Motion	EEC3	EEC3W	EEC4	EEC4W
Surge (m)	2.175	2.195	3.010	3.050
Heave (m)	1.205	1.200	1.640	1.470
Pitch (deg)	0.6242	0.5869	0.8175	0.8412
WEC2 rot. (deg)	6.5329	6.7657	7.3163	7.7980

Table 7. Statistical maximum value of motions for extreme conditions

Motion	EEC1	EEC1W	EEC2	EEC2W
Surge (m)	6.295	6.260	12.090	12.670
Heave (m)	3.175	3.150	4.590	4.320
Pitch (deg)	2.3556	2.3786	3.2990	3.2136
WEC2 rot. (deg)	15.952	18.352	18.815	22.767
Motion	EEC3	EEC3W	EEC4	EEC4W
Surge (m)	11.210	10.765	13.970	15.095
Heave (m)	4.455	4.180	5.530	5.015
Pitch (deg)	2.8528	2.3340	3.9885	4.9114
WEC2 rot. (deg)	18.156	20.503	20.885	24.380

A comparison of the spectra of surge (Fig. 7i), heave (Fig. 7ii) and pitch (Fig. 7iii) of the platform for all the examined extreme conditions is presented in Figure 7. For the motions of the platform, the peak of the spectra curves is observed close to the natural period of each motion as calculated by the decay tests (Table 4); when a second peak is occurred it is observed close to the frequency of the excitation wave. For surge motion an initial peak exists close to $\omega=0.05$ rad/sec induced by the resonance of the platform; in this frequency range the wind loading has significant effect (for the most of the examined conditions). For heave motion the peak of the spectra curve is obtained close to the frequency of the excitation waves. The effect of the wind loading on the spectra curves of the motions is insignificant for the EEC1W.

Table 8. Statistical mean value of motions for extreme conditions

Motion	EEC1	EEC1W	EEC2	EEC2W
Surge (m)	0.67	0.68	1.68	1.74
Heave (m)	0.06	0.09	0.05	0.04
Pitch (deg)	0.01	0.07	0.1	0.14
Motion	EEC3	EEC3W	EEC4	EEC4W
Surge (m)	1.01	1.25	2.28	2.49
Heave (m)	0.25	0.04	0.15	0.13
Pitch (deg)	0.08	0.16	0.13	0.22

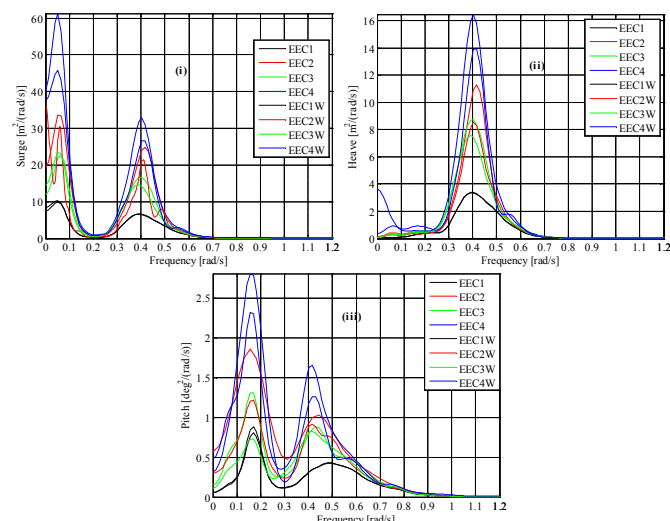


Figure 7. Comparison of spectra of surge (Fig. 7i), heave (Fig. 7ii) and pitch (Fig. 7iii) of semisubmersible platform

In Tables 9, 10 and 11 the one hour statistical std, max and mean of the experimental data for different structural responses for all the examined extreme conditions are presented. These responses are the tension of the mooring line ML2, the fore-aft tower base moment, MY, the axial internal load in one arm of WEC2, FZ, and the torque of WEC2. It should be noted that the torque at the rotation shaft is not measured directly. The torque is calculated by the summation of the bending moments MX1 and MX2 (Figure 5) at the lower ends of the two arms of each WEC. Ideally the torque at the axis of rotation for the survivability model of SFC should be zero. An increase of the std value of the tension of ML2 is obtained as a result of the wind loading. The opposite is observed for the bending moment of the tower. It should be noted that the maximum value of the tension of mooring line ML2 cannot be considered as the largest possible tension of the mooring lines. The largest mooring line tension is expected when the waves are against the mooring line ML1. For the internal loads of the WEC2 the effect of the wind loading is insignificant. The wind

loading results to the small increase of the mooring line tension. The largest max value that was measured experimentally is 3,031.87 kN for mooring line tension of ML2, 5,196.88 kNm for bending moment MY, 1,841.28 kNm for FZ internal load of one arm of WEC2 and 1,307.12 kNm for torque of WEC2 for EEC4W, EEC4, EEC3W and EEC4W conditions, respectively. The wind loading does not affect the mean value of the structural responses significantly. The mean value of torque and MY is equal to zero. It is noted that the tests are performed for representative operational and survival conditions for two sites of the MARINA Platform project; fatigue considerations for the mooring lines are out of the scopes of the present study.

Table 9. Statistical standard deviation value of different structural responses for extreme conditions

Structural response	EEC1	EEC1W	EEC2	EEC2W
ML2 tension (kN)	69.56	76.35	156.79	160.85
MY tower (kNm)	854.39	824.52	1,076.40	1,039.37
FZ WEC2 (kN)	105.59	103.15	124.76	124.27
Torque WEC2 (kNm)	EEC3	EEC3W	EEC4	EEC4W
Torque WEC2 (kNm)	133.77	139.25	138.92	140.63
Structural response	EEC3	EEC3W	EEC4	EEC4W
ML2 tension (kN)	119.80	124.29	106.05	126.52
MY tower (kNm)	966.25	879.62	1,050.64	978.56
FZ WEC2 (kN)	119.17	112.10	128.61	110.35
Torque WEC2 (kNm)	EEC3	EEC3W	EEC4	EEC4W
Torque WEC2 (kNm)	135.77	149.68	134.55	135.58

Table 10. Statistical maximum value of different structural responses for extreme conditions

Structural response	EEC1	EEC1W	EEC2	EEC2W
ML2 tension (kN)	2,229.77	2295.58	2761.89	2790.03
MY tower (kNm)	3,317.79	3105.15	4826.81	4377.97
FZ WEC2 k(N)	1,722.41	1705.25	1746.00	1772.53
Torque WEC2 (kNm)	1,074.69	1058.58	1105.73	1050.58
Structural response	EEC3	EEC3W	EEC4	EEC4W
ML2 tension (kN)	2,561.80	2,586.85	2,965.27	3,031.87
MY tower (kNm)	3,962.37	3,503.71	5,196.88	5,186.36
FZ WEC2 (kN)	1,781.87	1,841.28	1,833.95	1,781.07
Torque WEC2 (kNm)	1,051.12	1,224.98	978.05	1,307.12

Table 11. Statistical mean value of different structural responses for extreme conditions

Structural response	EEC1	EEC1W	EEC2	EEC2W
ML2 tension (kN)	1,765	1,765	1,785	1,794
FZ WEC2 (kN)	1,350	1,350	1,350	1,350
Structural response	EEC3	EEC3W	EEC4	EEC4W
ML2 tension (kN)	1,775	1,779	1,808	1,822
FZ WEC2 (kN)	1,350	1,350	1,350	1,350

COMPARISONS OBTAINED WITH THE SFC FUNCTIONALITY MODEL

For the functionality model of SFC both regular and irregular wave tests without and with wind loading have been conducted. Regular wave tests have been performed for a range of wave frequencies for estimating the RAOs of different response quantities of SFC. Regular wave tests with and without wind are executed; for the tests with wind the wind is aligned with the waves. Waves and wind propagate in the

positive surge direction (+X). Regular waves with twelve different wave periods are examined within the range 5.013 sec to 17.678 sec, while, the examined wave height, H_s , is equal to 2 m. During the regular waves with wind loading the wind speed is equal to $U_{wR}=9.35$ m/sec.

In Figure 8 the RAOs of surge, heave, pitch and rotation of WEC2 are plotted. It is noted that the unit of surge and heave motion of the platform is in m/m, the pitch is in deg/m and the rotation of WEC2 is in (degx0.1)/m. In general for all the motions of the platform the effect of the wind loading on the amplitude of RAOs is small. An increase of the examined wave period results to the increase of the RAOs of surge and heave motions. It must be noted that for the case of regular waves with wind loading the mean value of the surge (estimated by the time series of the motion) is 1.8 m higher compared to the mean value that the surge has for regular wave loading only. The amplitude of RAO and the mean value of the heave motion are not affected by the wind loading. The mean value of the amplitude of the pitch motion of the platform for the case of regular waves with wind loading is 2.2 degrees larger compared to the mean value for regular wave loading only. The wind loading results to the increase of the rotation of WEC2 compared to the case that only wave loading exists. This is attributed to the larger mean pitch value of the platform that has as a result leading WEC2 and WEC3 to be placed in higher positions in the vertical direction, closer to the MWL. In this case WEC2 and WEC3 are subjected to larger hydrodynamic loads. The resonance of the WEC2 rotation is observed for $T=14.7$ sec.

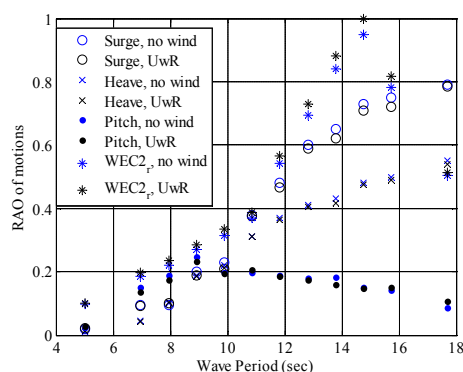


Figure 8. Comparison of RAO of surge, heave, pitch and rotation of WEC2

The operational environmental conditions of the functionality model of SFC are tabulated in Table 12. As far as the tests with wave and wind loading, OEC1W ~ OEC3W, the turbulence intensity of the measured wind data is 0.009. The mean value of the thrust force (shear load at the tower top) is equal to 647.5 kN for all the examined operational conditions.

Table 12. Examined operational environmental conditions in full scale values

Operational conditions/Test cases	H_s (m)	T_p (sec)	U_w (m/sec)
OEC1	3.0	7.0	-
OEC2	3.0	9.0	-
OEC3	3.0	12.0	-
OEC1W	3.0	7.0	9.35
OEC2W	3.0	9.0	9.35
OEC3W	3.0	12.0	9.35

In Tables 13, 14 and 15 the one hour statistical std, max and mean of the experimental data for different structural responses for all the

examined operational conditions are presented.

As far as the std value, an increase is obtained mainly for MY of tower and torque of WEC2 responses. With regard to the maximum value of the responses, the wind loading results in a significant increase of surge and pitch of the platform and of the MY of tower. The wind loading affects the mean value of the surge and pitch of the platform. For the examined operational conditions the mean value of the surge and pitch motion for OEC1W, OEC2W and OEC3W are 1.8 m and 2.1 deg larger compared to OEC1, OEC2 and OEC3, respectively; this is attributed to the wind loading. In Figure 9 spectra comparison of experimental responses of different parts of SFC are plotted. As far as the motions of the platform, the resonance of each motion spectrum is occurred for the motion's natural frequency as calculated by the decay tests. The second peak in the motion curves exists close to the frequency of wave excitation. The effect of the wind loading is significant for pitch motion while it is smaller for surge motion. The effect of the wind loading is mainly observed for frequencies close to the natural frequencies of the motions of the platform. Regarding the bending moment MY the resonance of the curve exists close to the first bending eigenfrequency of the tower ($\omega=3.8$ rad/sec) and only for conditions with wind loading.

For both structural responses of WEC2, FZ and torque, the resonance is occurred close to the frequency of wave excitation. The effect of the wind loading is small for both structural responses.

Table 13. Standard deviation values of different structural responses for operational conditions

Response	OEC1	OEC1W	OEC2	OEC2W
Surge (m)	0.542	0.5914	0.373	0.397
Pitch (deg)	0.234	0.201	0.216	0.1825
MY tower (kNm)	674.83	1,286.48	571.62	1,242.39
FZ WEC2 (kN)	72.39	74.67	71.02	68.62
Torque WEC2 (kNm)	1,137.34	1,155.3	1,207.4	1,321.04
Response	OEC3	OEC3W		
Surge (m)	0.375	0.668		
Pitch (deg)	0.175	0.189		
MY tower (kNm)	384.8	1,198.5		
FZ WEC2 (kN)	54.93	53,382		
Torque WEC2 (kNm)	1,233.9	1,436.86		

Table 14. Maximum values of different structural responses for operational conditions

Response	OEC1	OEC1W	OEC2	OEC2W
Surge (m)	2.02	4.066	1.73	4.158
Pitch (deg)	0.85	2.983	1.033	3.007
MY tower (kNm)	3,199	4,682.3	2,308.1	4,310.5
FZ WEC2 (kN)	1,578.3	1,588	1,603.8	1,581.03
Torque WEC2 (kNm)	2,132.6	2,169.3	2,540.3	2,746.99
Response	OEC3	OEC3W		
Surge (m)	1.48	3.369		
Pitch (deg)	0.87	2.945		
MY tower (kNm)	1,566.5	3,582.9		
FZ WEC2 (kN)	1,550.2	1,553.1		
Torque WEC2 (kNm)	2,470.6	2,829.7		

Table 15. Mean values of different structural responses for operational conditions

Response	OEC1	OEC1W	OEC2	OEC2W
Surge (m)	0.86	2.59	0.76	2.848
Pitch (deg)	0.04	2.166	0.027	2.145
MX tower (kNm)	0.15	0.05	0.37	0.41
FZ WEC2 (kN)	1,350	1,350	1,350	1,350
Torque WEC2 (kNm)	0.27	0.33	0.51	0.29
Response	OEC3	OEC3W		
Surge (m)	0.552	2.39		
Pitch (deg)	0.023	2.141		
MX tower (kNm)	0.027	0.285		
FZ WEC2 (kN)	1,350	1,350		
Torque WEC2 (kNm)	0.225	1.22		

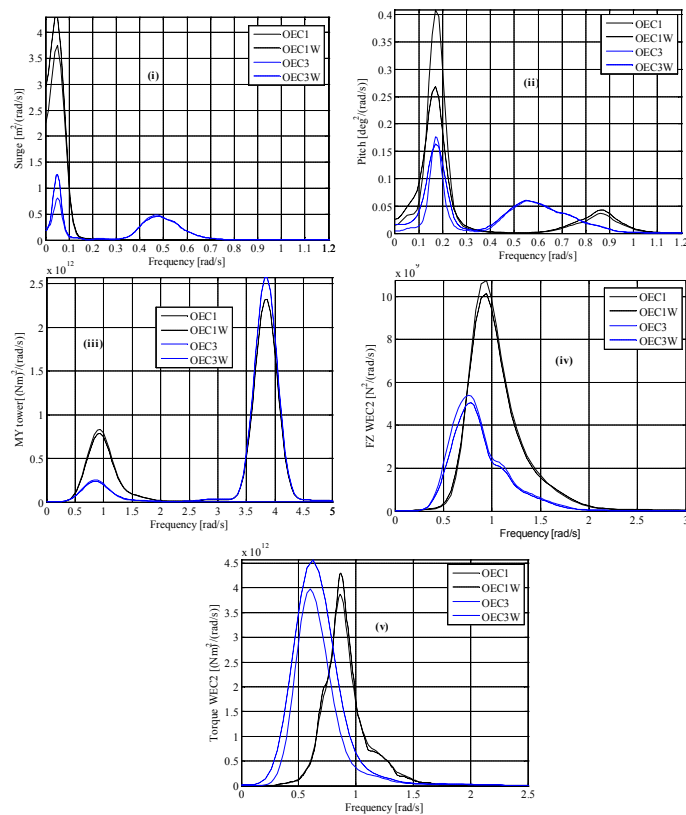


Figure 9. Comparison of spectra of surge (Fig. 9i), pitch (Fig. 9ii), MY tower base moment (Fig. 9iii), FZ internal load of one arm of WEC2 (Fig. 9iv) and torque of WEC2 (Fig. 9v)

As far as the functionality of the WECs of SFC, in Figure 10 bar plots of statistical quantities (mean, std and max) of the one hour time series of the produced power of WEC2 are plotted. An increase of the produced power is observed moving from OEC1 to OEC3 since the period of wave excitation is closer to the natural period of rotation of WECs. The largest measured mean produced power is 70.2 kW for OEC3W.

On average a 6% increase of the produced power exists for the conditions with wind loading compared to the conditions without wind loading. This is attributed to the larger rotation of the WECs. For

conditions with wind loading the mean value of the pitch of the platform is larger compared to the case without wind loading and the two WECs, WEC2 and WEC3, are getting into higher position (close to the mean water level) and one is getting into a lower position due to wind overturning moment. The net effect is that the two WECs are subjected to larger hydrodynamic loading. It should be noted that the produced power of WECs is not optimum; the experimental study of SFC is not dealing with the maximization of the produced power but with the proof of the combined concept SFC. Larger amount of produced power can be achieved with geometry optimization of the flaps and with an appropriate control scheme for the operation of the PTO configuration. It should be noted that combining the flap-type WECs with the floating wind turbine was found to have insignificant effect on the wind power production but increases the total power production by 3~5% (Michailides et al. 2014). However, based on a preliminary evaluation in the MARINA project (Soho and Auer, 2014) the cost of energy for the SFC is higher than that of a pure semisubmersible wind turbine.

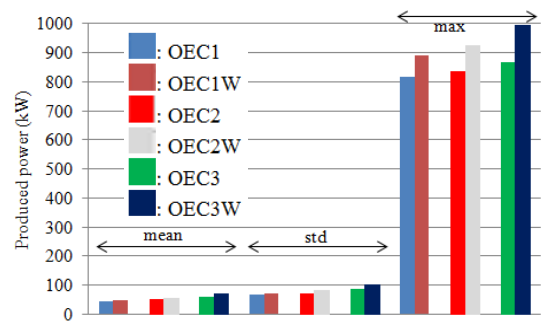


Figure 10. Comparison of statistical mean, std and max value of the produced wave power of WEC2.

CONCLUSIONS

In the present paper wave-induced responses are compared with wave-wind-induced responses based on experiments of the combined wind/wave energy concept SFC. The comparison is conducted for two different experimental campaigns of SFC. The survivability and the functionality physical model campaigns of SFC for extreme and operational environmental conditions, respectively. The experiments of the SFC are conducted in an 1:50 scale physical model in ECN's ocean basin.

For the survivability physical model of SFC, the effect of the wind loading is significant for the maximum value of the surge motion of the platform and for the rotation of the WEC2. The largest values of the motions are occurred for wave with wind loading conditions. The structural responses of mooring lines and tower's bending moment are affected by the wind loading, while, the structural responses related with the WEC2 are not affected by the wind loading.

With regard to the functionality model and regular wave tests, the RAOs of the motions of the platform are not affected by the wind loading significantly. For the irregular tests the effect of the wind loading is large for pitch motion while is small for surge motion. Wind loading dominates the response of tower's bending moment. The effect of the wind loading in structural responses of different parts of WECs is small. A small increase of the produced power of the WECs exists for conditions with wind loading.

The model tests are conducted with a constant and uniform wind field; if a turbulent wind field is considered more significant dynamic response induced by wind is expected. Finally it will be interesting to study the potential of reducing the cost of combined concepts by the use of appropriate optimization techniques.

ACKNOWLEDGEMENTS

The authors would like to acknowledge the financial support from the MARINA Platform project (Marine Renewable Integrated Application Platform, Grant Agreement no. 241402) under the European Community FP7 Energy Programme. The contribution of Thomas Soulard and Sylvain Bourdier at ECN to the planning, construction and execution of the model tests is highly appreciated. The financial support from the Research Council of Norway through the Centre for Ships and Ocean Structures and the Centre for Autonomous Marine Operations and Systems, the Norwegian University of Science and Technology, is also acknowledged.

REFERENCES

- Azcona, J, Bouchotrouch, F, González, M, Garcíandía, J, Munduate, X, Kelberlau, F, and Nygaard, T.A (2014). "Aerodynamic Thrust Modelling in Wave Tank Tests of Offshore Floating Wind Turbines Using a Ducted Fan," *Journal of Physics: Conf. Series*, 524, 012089.
- Chung, J.S. (1976). "Motion of a Floating Structure in Water of Uniform Depth," *Journal of Hydronautics*, 10(3), 65-73.
- Chung, J.S. (1994). "Added Mass and Damping on an Oscillating Surface-Piercing Circular Column with a Circular Footing," *International Journal of Offshore and Polar Engineering*, 4(1), 11-17.
- Courbois, A (2013). "Etude expérimentale du comportement dynamique d'une éolienne offshore flottante soumise à l'action conjuguée de la houle et du vent," Ph.D. thesis, Ecole Centrale de Nantes (in French).
- Flocard, F, and Finnigan, T.D. (2010). "Laboratory experiments on the power capture of pitching vertical cylinders in waves," *Ocean Engineering*, 37, 989-997.
- Fowler, M.J., Kimball, R.W., Thomas, D.A., and Goupee, A.J (2013). "Design and Testing of Scale Model Wind Turbines for Use in Wind/Wave Basin Model Tests of Floating Offshore Wind Turbines," *32nd International Conference on Ocean, Offshore and Arctic Engineering-OMAE 2013*, OMAE2013-10122, Nantes, France.
- Gao, Z, Moan, T, Wan, L, and Michailides, C (2016). "Comparative numerical and experimental study of two combined wind and wave energy concepts," *Journal of Ocean Engineering and Science*, 1, 36-51.
- Jonkman, J, Butterfield, S, Musial, W, and Scott, G (2009). "Definition of a 5-MW Reference Wind Turbine for Offshore System Development," *National Renewable Energy Laboratory*, Technical Report, NREL/TP-500-38060, Boulder.
- Jonkman, J.M., and Matha, D (2011). "Dynamics of offshore floating wind turbines-analysis of three concepts," *Wind Energy*, 14(4), 557-569.
- Karimirad, M, and Michailides, C (2015). "V-shaped semisubmersible offshore wind turbine: An alternative concept for offshore wind technology," *Renewable Energy*, 83, 126-143.
- Li, L, Gao, Z, and Moan, T (2015). "Joint Distribution of Environmental Condition at Five European Offshore Sites for Design of Combined Wind and Wave Energy Devices," *Journal of Offshore Mechanics and Arctic Engineering*, 137, 031901-1.
- World Energy Council (2013). "World Energy Perspective: Cost of Energy Technologies", ISBN: 978 0 94612 130 4.
- MARINA Platform (Online). Available at: <http://www.marina-platform.info/index.aspx> [Accessed in December 2015].
- Martin, H.R., Kimball, R.W., Viselli, A.M., and Goupee, A.J (2012). "Methodology for Wind/Wave Basin Testing of Floating Offshore Wind Turbines," *31st International Conference on Ocean, Offshore and Arctic Engineering-OMAE 2012*, OMAE2012-83627, Rio de Janeiro, Brazil.
- Michailides, C (2015). "Power Production of the Novel WLC Wave Energy Converter in Deep and Intermediate Water Depths," *Recent Patents on Engineering*, 9, 42-51.
- Michailides, C, and Angelides, D.C (2015). "Optimization of a flexible floating structure for wave energy production and protection effectiveness," *Engineering Structures*, 85, 249-263.
- Michailides, C, Luan, C, Gao, Z, and Moan, T (2014). "Effect of Flap Type Wave Energy Converters on the Response of a Semi-submersible Wind Turbine in Operational Conditions," *32nd International Conference on Ocean, Offshore and Arctic Engineering-OMAE 2014*, OMAE2014-24065, pp. V09BT09A014.
- Michailides, C, Gao, Z, and Moan, T (2015). "Response Analysis of the Combined Wind/Wave Energy Concept SFC in Harsh Environmental Conditions," *Renewable Energies Offshore*, Edited by C. Guedes Soares, CRC Press 2015, Pages 877-884, eBook ISBN: 978-1-315-64785-2, DOI: 10.1201/b18973-123
- Michailides, C, Gao, Z, and Moan, T (2016a). "Experimental and numerical study of the response of the offshore combined wind/wave energy concept SFC in extreme environmental conditions," *Marine Structures*, 50, 35-54.
- Michailides, C, Gao, Z, and Moan, T (2016b). "Experimental Study of the Functionality of a Semisubmersible Wind Turbine Combined with Flap-Type Wave Energy Converters," *Renewable Energy*, 93, 675-690.
- Muliawan, M.J., Karimirad, M, and Moan, T (2013). "Dynamic response and power performance of a combined spar-type floating wind turbine and coaxial floating wave energy converter," *Renewable Energy*, 50, 47-57.
- Müller, K, Sandner, F, Bredmose, H, Azcona, J, Manjock, A, and Pereira, R (2014). "Improve Tank Test Procedures for Scaled Floating Offshore Wind Turbines," *The International Wind Engineering Conference – Support Structures & Electrical Systems*, Hannover, Germany.
- Ogai, S, Umeda, S, and Ishida, H (2010). "An experimental study of compressed air generation using a pendulum wave energy converter," *Journal of Hydrodynamics*, 22(5), 290-295.
- Olav Olsen AS (Online). Available at: <http://www.olavolsen.no/node/82> [Accessed in December 2015].
- O'Sullivan, K, and Murphy, J (2013). "Techno-Economic Optimisation of an Oscillating Water Column Array Wave Energy Converter," *Proceedings of the 10th European Wave and Tidal Energy Conference*, Aalborg, Denmark.
- Pecher, A, Kofoed, J.P., Espedal, J, and Hagberg, S (2010). "Results of an experimental study of the langlee wave energy converter," *20th International Offshore and Polar Engineering Conference*, ISOPE, Beijing, China.
- Roddi, D, Cermelli, C, Aubault, A, and Weinstein A (2010). "WindFloat: A floating foundation for offshore wind turbines," *Journal of Renewable and Sustainable Energy*, 2(3).
- Sojo, M. and Auer, G. (2014) D1.12 – Final Summary Report. EU FP7 MARINA Platform Project. Acciona Energia.
- Wan, L, Gao, Z, Moan, T (2015). "Coastal Engineering, Experimental and Numerical Study of the Hydrodynamic Responses of a Combined Wind and Wave Energy Converter Concept in Survival Modes," *Coastal Engineering*, 104, 151-169.
- Wan, L, Gao, Z, Moan, T, and Lugni, C (2016). "Comparative experimental study of the survivability of a combined wind and wave energy converter in two testing facilities," *Ocean Engineering*, 111, 82-94.